Journal of Industrial and Engineering Chemistry xxx (xxxx) xxx

Contents lists available at ScienceDirect

Journal of Industrial and Engineering Chemistry

journal homepage: www.elsevier.com/locate/jiec

Modeling of Cu(II) adsorption on the activated *Phragmites australis* waste by fuzzy-based and neural network-based inference systems

Oğuzcan Elver [a], Fulya Aydın Temel [b,*], Ozge Cagcag Yolcu [c], Feryal Akbal [a], Ayşe Kuleyin [a]

[a] Department of Environmental Engineering, Faculty of Engineering, Ondokuz Mayıs University, Samsun, 55200, Turkey
[b] Department of Environmental Engineering, Faculty of Engineering, Giresun University, Giresun, 28200, Turkey
[c] Department of Statistics, Faculty of Sciences and Arts, Marmara University, İstanbul, 34722, Turkey

ARTICLE INFO

Article history:
Received 12 October 2022
Revised 12 July 2023
Accepted 15 August 2023
Available online xxxx

Keywords:
Adsorption
Soft computing
Feed Forward Neural Network
Mamdani Fuzzy Inference System
Genetic Algorithm

ABSTRACT

In this study, soft computing models were used to predict Cu(II) adsorption on activated *Phragmites australis* waste (PAC) and commercial activated carbon (CAC). The effects of pH, adsorbent dose, contact time, initial concentration, and temperature were evaluated in batch mode. Cu(II) adsorption of both adsorbents was better described by the pseudo-second-order kinetic and Langmuir isotherm models. The maximum adsorption capacity was found as 48.31 mg/g and 45.46 mg/g for PAC and CAC, respectively. From thermodynamics, Cu(II) adsorption onto PAC and CAC had an exothermic, randomness, feasible, and spontaneous nature, as physical adsorption. Desirability levels were above 90% in the optimization of the adsorbent parameters that constitute the Mamdani Fuzzy Inference System (MFIS) and Feed-Forward Neural Network (FFNN) inputs. FFNN and MFIS showed superior prediction performance with an error percentage of less than 1% in 2 of 6 experimental designs and were successful with a percentage error of approximately 2–3% in 2 of them. In others, the error percentage of 6–8% was at a level that indicates acceptable and competitive prediction performance. As a result of the hypothesis tests, it was proven that there was no statistically significant difference between PAC and CAC.

Introduction

Copper is one of the most frequently encountered heavy metal pollutants, which are released as a result of industrial activities. Copper is important for human life, but its excessive intake causes health problems such as kidney deformation, anemia, gastrointestinal problems, and lung cancer. Therefore, the drinking water standard set by USEPA is a maximum of 1.3 ppm [1–3]. Different technologies such as chemical precipitation, membrane processes, advanced oxidation, and adsorption are applied to remove heavy metals from wastewater. The adsorption process that does not produce toxic sludge, is more economical and simple operating, achieves high removal efficiency, and is a better option in heavy metal removal as an environmentally friendly old technology used in water and wastewater treatment [4–6]. In recent years, many studies have been performed to find materials that are low-cost and easily available locally as an alternative to the activated carbon frequently used in the adsorption process. Some of them are agro-industrial wastes [7–9], natural materials [6,10,11], biopolymers [12,13], and nanoparticles [14–17]. Studies have been carried out to use them as an alternative sorbent for the removal of various pollutants, instead of being disposed of due to a large number of agricultural wastes and their easy availability, their cheap, renewable, and high carbon contents [18–21]. Moreover, the preparation of activated carbon which has a porous structure, mechanical strength, and high adsorption capacity from agricultural wastes, and its usage to remove different types of pollutants in water/wastewater were reported by some researchers [22–27].

In this study, harvest wastes of the *Phragmites australis* plant, which is very abundant and is considered waste nowadays, and the use of activated carbon obtained from these wastes as an alternative adsorbent were investigated for Cu(II) removal. Various agro-wastes have been evaluated for Cu(II) removal from aqueous solutions/wastewaters but before, the activated *Phragmites australis* has been used in very few studies. Reuse of *Phragmites australis* waste will reduce the amount of solid waste that needs to be managed. In addition, the success achieved in the removal of special pollutants in aquatic environments will also contribute to the improvement of water quality. The reuse of these wastes is very important to prevent potential environmental pollution.

* Corresponding author.
E-mail address: fulya.temel@giresun.edu.tr (F. Aydın Temel).

https://doi.org/10.1016/j.jiec.2023.08.031
1226-086X/

Statistical-based approaches such as Response Surface Methodology (RSM) have been usually applied to model the adsorption process under changing operating conditions [28,29]. However, in recent years, artificial neural networks (ANNs) as a soft computing technique, that can reveal non-linear relationships between inputs and outputs based on machine learning, and can procure appropriate models by learning the data structure, especially by their hidden layers. Although artificial neural networks have been applied in many studies for the evaluation of time-dependent data [30,31], they have been the subject of a limited number of studies in the literature for modeling and optimization of the adsorption process [32–39]. Fuzzy inference systems (FIS) is also another soft computing technique. Although not very common in the literature, adaptive neuro-fuzzy inference systems (ANFIS) were used for some pollutant removal in modeling the adsorption process [40–43]. In this study, Cu(II) adsorption performances of activated *Phragmites australis* waste and commercial activated carbon were modeled by using Feed-Forward Neural Networks (FFNN) and Mamdani Fuzzy Inference Systems (M−FIS) which have almost never been applied in the adsorption process. The nonlinear relations by FFNN and fuzzy relations with MFIS were modeled and modeling performances were evaluated in terms of root mean square error (RMSE), median absolute percentage error (MdAPE), median absolute error (MdAE) performance criteria, unlike the other modeling tools. Moreover, the soft computing models used as prediction tools are simulations of the process, the process parameters were optimized through these simulations by Genetic Algorithm (GA).

The present study was performed to understand the adsorption mechanisms of activated Phragmites australis (PAC) and commercial activated carbon (CAC) for Cu(II) removal from aqueous solutions and to predict and optimize the Cu(II) adsorption process by using feed-forward neural networks (FFNN) and Mamdani fuzzy inference systems (M−FIS). The scopes of the present study were as follows: (*i*) to understand the Cu(II) adsorption mechanism by kinetic and isotherm models, (*ii*) to decide the adsorption suitability by the thermodynamic parameters, (*iii*) to compare Cu(II) removal performances of both adsorbents, (*iv*) to prove the prediction abilities of soft computing based prediction models; (*v*) to compare the model results by RMSE, MdAPE, and MdAE, (*vi*) to evaluate the performances via some properties of regression analysis; and (*vii*) to optimize the outputs of the best model.

Materials and methods

Materials

Phragmites australis waste was obtained from the villagers engaged in the reed trade. *Phragmites australis* were collected from the Kızılırmak Delta in Bafra plain westerly of Samsun, Turkey. The dried reed plants in air seasoning were ground in a mill and sieved. Particles in the range of 0.425–0.600 mm were used to produce the activated carbon. The sieved biomass in the range of 0.425–0.600 mm was placed in a specially-made reactor. The reactor was a stainless steel cylinder with dimensions of 4.5 cm diameter, 8.30 cm in-depth, and 0.5 cm wall thickness. The carbonization process was carried out at 600 °C of temperature for 1 h. It was taken into a closed combustion reactor during the carbonization process to be activated with 99.0% NaOH (Merck) at a ratio of 1:3. The obtained product was washed with distilled water to decrease pH value from 13 to 6–7, and dried in the oven at 105 °C for 24 h [44]. The obtained product was coded as "PAC".

The other adsorbent used in the study was commercial active carbon (CAC) (Merck). CAC had 12.01 g/mol of molecular mass and was produced by activating coal. Synthetic wastewater was prepared by using $CuSO_4.5H_2O$ (Merck) in analytical grade.

Methods

The effects of adsorbent dose, pH, contact time, initial concentration, and temperature on Cu(II) adsorption capacities of PAC and CAC were investigated by the batch equilibrium technique. Experiments were performed with 100 mg/L synthetic wastewater at a stirring speed of 150 rpm using an orbital mixer (JULABO SW22) at room temperature. The phases of the mixture were separated by using 0.45 μm of filter paper. Cu(II) concentration was analyzed by an atomic adsorption spectrophotometer (HACH LANGE DR6000). The removal efficiency (RE) and the amount of Cu(II) adsorbed per gram adsorbent were calculated by Eqs. (1) and (2), respectively.

$$RE(\%) = \frac{C_t - C_0}{C_0} \times 100 \tag{1}$$

$$q = \frac{(C_0 - C_t)V}{M} \tag{2}$$

where, C_0 is the initial Cu(II) concentration (mg/L), C_t is Cu(II) concentration in t time, M is the adsorbent amount (g), V is the wastewater volume (L), and q is the quantity of the adsorbate exchanged per unit mass of the adsorbent.

Kinetic and isotherm models

Kinetics

Elovich model expresses chemisorption that occurs on adsorbent materials with heterogeneous structures. Its linear equation is given in Eq. (3). α is the chemisorption rate (mg/g min), β is a coefficient related to the surface coverage and activation energy for chemisorption (g/mg), t is contact time (min), q_t is the sorption capacity of adsorbents (mg/g) [6],

$$q_t = \frac{1}{\beta}\ln(\alpha\beta) + \frac{1}{\beta}lnt \tag{3}$$

The intraparticle diffusion model explains the adsorbate transfer to the adsorbent particles [45]. In Eq. (4), k_{id} is the rate constant (mg/g $h^{1/2}$), C is a coefficient related to the boundary layer dimension, q_t is the sorption capacity of adsorbents (mg/g), and t is contact time (h).

$$q_t = k_{id}t^{1/2} + C \tag{4}$$

Pseudo first-order reaction model assumes that the physical adsorption and the occupancy rate of the adsorption zones in the adsorbent are directly proportional to the number of unused zones [46]. The linear equation is given in Eq. (5). Here, q_t is the sorption capacity of adsorbents (mg/g), q_e, is the equilibrium sorption capacity of adsorbents (mg/g), k_1 is the rate coefficient of Lagergreen (1/min), and t is contact time (min).

$$ln(q_e - q_t) = lnq_e - k_1 t \tag{5}$$

Pseudo second-order reaction model assumes that chemical sorption is dominant by using electron exchange between the sorbate and the sorbent in the sorption process [47]. The linear equation is presented in Eq. (6). Here, q_t is the sorption capacity of adsorbents (mg/g), q_e, is the equilibrium sorption capacity of adsorbents (mg/g), k_2 is the adsorption velocity constant of the model (g/mg min), h is the inlet sorption ratio (mg/g min) and t is contact time (min) (Eq. (7)).

$$\frac{t}{q_t} = \frac{1}{k_2.q_e^2} + \frac{t}{q_e} \tag{6}$$

$$h = k_2.q_e^2 \tag{7}$$

Isotherms

Langmuir model assumes that the sorption process is homogeneous, monolayer, and energetically equivalent on the adsorbent surface [48]. The model equation is given in Eq. (8). Here, q_e, is the equilibrium sorption capacity of adsorbents (mg/g), K_L is a model constant that gives the measurement of the affinity between adsorbate and adsorption sites (L/mg), C_e is the concentration of adsorbate (mg/L), C_0 is inlet concentration of adsorbate (mg/L), q_m is the calculated sorption capacity of adsorbents (mg/g), and R_L is a separation factor that uses to explain the interaction between the adsorbent and adsorbate (dimensionless) (Eq. (9)).

$$\left(\frac{C_e}{q_e}\right) = \left(\frac{1}{q_m K_L}\right) + \left(\frac{C_e}{q_m}\right) \tag{8}$$

$$R_L = \frac{1}{(1 + K_L C_0)} \tag{9}$$

Freundlich model assumes that the sorption process is heterogeneous, the exponential distribution of active sites and their energies on the adsorbent surface [49]. The linear equation is given in Eq. (10). Here, q_e is the equilibrium sorption capacity of adsorbents (mg/g), C_e is the concentration of adsorbate (mg/L), K_F is a constant related to the adsorbent capacity (mg/g), n gives the adsorption intensity dependent on the degree of heterogeneity (L/g).

$$\log q_e = \log K_F + \left(\frac{1}{n}\right) \log C_e \tag{10}$$

Tempkin model assumes that the adsorption process is uniformly distributed and the heat of adsorption of molecules decreases linearly [50]. The linear equation is shown in Eq. (11). Here, C_e is the concentration of adsorbate (mg/L), q_e is the equilibrium sorption capacity of adsorbents (mg/g), R is the gas coefficient (8.3145 J/mol K), T is the solution temperature (K), b is a constant dependent on the adsorption heat(J/mol), K_T is the equilibrium binding coefficient related to the binding energy.

$$q_e = \frac{RT}{b} lnK_T + \frac{RT}{b} lnC_e \tag{11}$$

Dubinin–Radushkevich model is a general isotherm model used to test the adsorption nature. The empirical equations are listed in Eqs. (12) and (13) [10]. Here, q_e is the equilibrium sorption capacity of adsorbents (mg/g), q_m is the equilibrium sorption capacity of adsorbents (mg/g), β is a coefficient based on the adsorption energy (mol^2/kj^2), ε is Polanyi potential based on the equilibrium adsorbate concentration, R is the gas coefficient (8.3145 J/mol K), T is the solution temperature (K), C_e is the concentration of adsorbate (mg/L)

$$lnq_e = lnq_m - \beta\varepsilon^2 \tag{12}$$

$$\varepsilon = RTln\left(1 + \frac{1}{C_e}\right) \tag{13}$$

Soft computing

The concept of soft computing (SC) introduced by Zadeh [51], unlike traditional computing, deals with approximate models and offers satisfactory solutions for complex real-life problems. Opposite to hard computing (HC), soft computing takes a flexible approach to imprecision, uncertainty, and partial truth in problems. The SC generally includes techniques such as fuzzy logic, genetic algorithms, and artificial neural networks [52]. While the HC modeling process is based on numerical modeling, the SC modeling process is based on approximate modeling. The flow chart for soft computing–based prediction models was given in Fig. 1.

Artificial neural networks - Feed Forward Neural Networks

An artificial neural network is a soft computing technique that reflects the behavior of the human brain, allowing the modeling

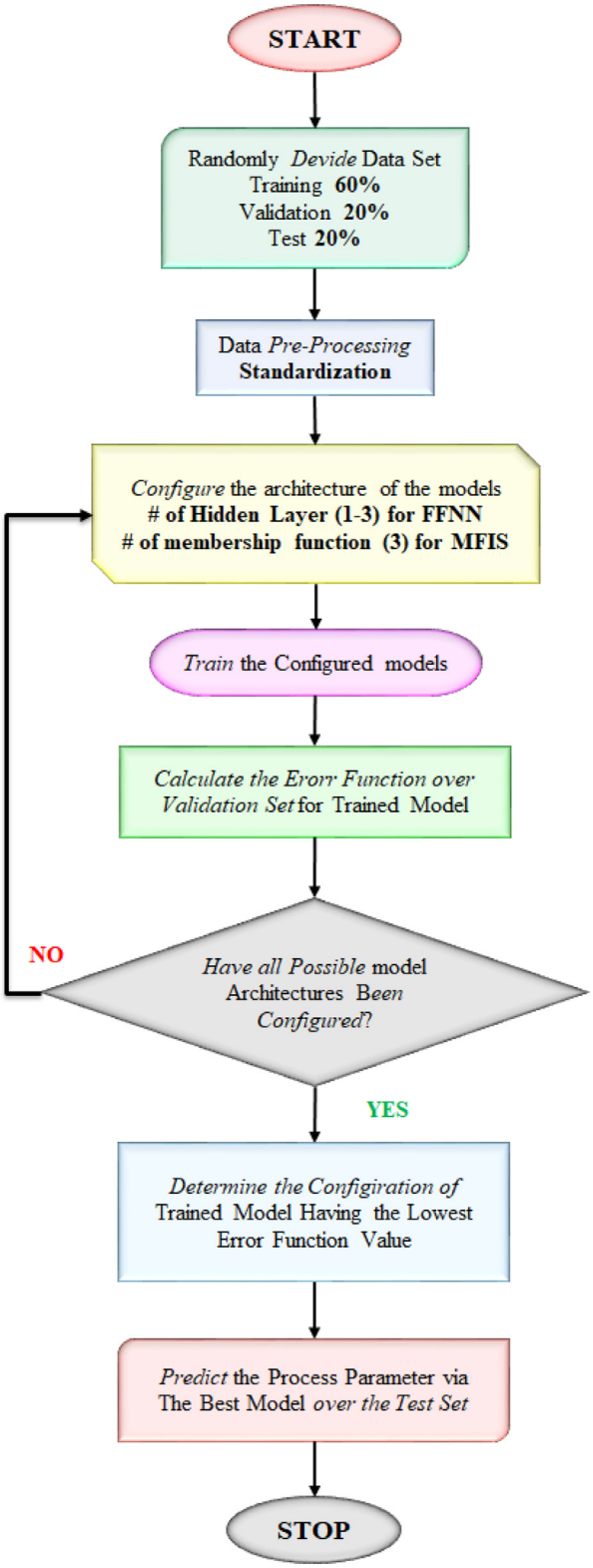

Fig. 1. Flow chart for soft computing–based prediction models.

mechanism to recognize patterns and solve problems in various fields. The most common ANN kind is Feed-Forward Neural Network as a multilayer perceptron neural network introduced by Werbos [53] and improved by Rumelhart et al. [54]. FFNN has no mechanism that includes loops and is called feed-forward because information only moves forward in the network.

Mamdani fuzzy inference systems

In a special issue or problem, reaching a particular result based on specific pieces of evidence associated with logic can be described as inference. Fuzzy inference systems are based on fuzzy logic and are widely used for various problems such as prediction, modeling, and process control. Mamdani fuzzy inference systems (MFISs) proposed by Mamdani [55] operate the inference process based on rules supplied by experienced human operators or by internal relations of data.

Genetic algorithm

In this study, after fitting both soft computing prediction tools to data patterns, the parameter values that would yield the highest adsorption rates have been reached with the genetic algorithm (GA), developed by John Holland [56] and improved by De Jong [57], via an optimization process. The GA based on natural selection is a soft computing technique for solving both constrained and unconstrained optimization problems.

Results and discussions

Effects of pH, adsorbent dose, and contact time

In addition to affecting the physicochemical structure of adsorbents, it is known that the solution pH value significantly affects the behavior of metal ions in aqueous media such as redox reactions, precipitation, hydrolysis, complexation with ligands, and thus the adsorption behavior of metal ions [11,16,58]. In this study, the effects of initial pH on Cu(II) adsorption by PAC and CAC adsorbent materials were performed to determine the optimum pH value. The works were conducted by different pH values (3.01, 5.07, 7.25, and 9.05) of the solution containing 100 mg/L Cu(II) ion with adsorbent doses of 6 g/L at room temperature and 200 rpm for 1 h. The initial pH value of the Cu(II) solution was determined as 5.07 and pH adjustment was made by using 1 M H_2SO_4 and NaOH solutions for the others. Fig. 2(a) shows the effects of initial pH values for Cu(II) adsorption on both adsorbents. From Fig. 2(a), the adsorption capacity of both adsorbent materials increased with the increase of initial pH. At pH 7.25, the removal efficiencies of PAC and CAC were determined as 96.78 and 96.85%, respectively. The Cu(II) adsorption of PAC and CAC was not significantly changed with the increasing pH. At the first pH value of the Cu(II) solution, the removal efficiencies were 80.57% for PAC and 88.44% for CAC. The studies focused on Cu(II) removal with different adsorbents have reported that the removal efficiencies reach the optimum level when the initial pH value of the solution was in the range of 5–7 [5,59]. The obtained results for both adsorbents conformed to the previous studies. According to the results obtained from the experiments for both adsorbents, pH 5 and 7 were used for all further experiments. Thus, the adsorption capacities of both adsorbent materials at both pH values were compared.

Another parameter affecting the adsorption process is the adsorbent amount. The effect of different applied amounts of both adsorbents on Cu(II) removal was investigated and compared. The effectiveness of 10 different adsorbent doses ranging from 0.5 to 8 g/L on Cu(II) removal was determined as results of studies carried out at a stirring speed of 200 rpm, room temperature, pH 5, pH 7 for 1 h with 100 mg/L of initial concentration and presented in Fig. 2(b). Cu(II) removal increased with increasing the amount of both adsorbents from 0.5 g/L to 8 g/L. This increase can be explained directly related to the increase in the contact surface [60,61]. As a result of the studies conducted with both PAC and CAC at pH 5, it was observed that Cu(II) removal increased rapidly up to 6 g/L, and then the increase slowed down. At this pH value, removal efficiencies for 6g/L of adsorbent dose were determined as 80.43% for PAC and 89.54% for CAC. Similarly, in the experiments performed in pH 7, the adsorption performances of both adsorbents increased rapidly until a dose of 3 g/L, however, there was no significant rise in Cu(II) removal efficiencies with an increasing dose. The removal efficiencies determined at pH 7 and 3 g/L of adsorbent doses were 80.01 and 92.27% for PAC and CAC, respectively. When the amounts of Cu(II) adsorbed per unit weights of the adsorbents were evaluated, they were calculated as 0.67 mg/g and 0.75 mg/g for PAC and CAC, respectively with 6 g/L of adsorbent dose at pH 5. At 3 g/L of adsorbent dose and pH 7, these values were found to be 1.29 mg/g and 1.48 mg/g, respectively. Cu(II) adsorption was not changed significantly between 6 g/L and 8 g/L of adsorbent doses at pH 5, and 3 g/L and 8 g/L of adsorbent doses at pH 7. The reason for this was that almost all Cu(II) ions bind to the adsorbents and equilibrium was established between Cu(II) ions bound to the adsorbent and Cu(II) ions in the solution [58]. Hence, the optimum adsorbent doses of PAC and CAC at pH 5 and 7 were selected as 6 g/L and 3 g/L for subsequent experiments, respectively.

The effects of contact time ranging between 10 and 240 min on Cu(II) adsorption for both adsorbents were carried out to determine the equilibrium time at room temperature, stirring speed of 200 rpm, initial Cu(II) concentration of 100 mg/L, the optimum pH values, and with the optimum adsorbent doses (Fig. 2(c)). The removal efficiencies and the amount of removed substance per unit adsorbent (q_t) increased in the first 60 minutes for both pH values and both adsorbents. Between the 60^{th} and 240^{th} minutes, the q_t value remained constant, that is, there were no important improvements in adsorption processes. When q_t values were evaluated at pH 5 and 60^{th} min, they were found as 15.76 mg/g and 17.21 mg/g for PAC and CAC, respectively. At pH 7, these values were calculated as 29.18 mg/g for PAC and 32.71 mg/g for CAC, and an increase in q_t values was observed. As seen in Fig. 2(c), although the equilibrium times of both adsorbents were the same at the optimum pH values, the amount of adsorbed Cu(II) ions per unit adsorbents increased approximately twice. Similarly, it was determined that the removal efficiencies were approximately the same for both adsorbents at both pH values with the increase in contact time. The removal efficiencies were 82.50% for PAC and 90.10% for CAC at pH 5 while these values were calculated as 82.58% and 92.57% at pH 7, respectively. Therefore, the removal and q_t values at 60^{th} min were given as equilibrium values.

Effect of temperature

It is known that the amount of Cu(II) adsorbed varies depending on the initial ion concentration. The adsorption performances of PAC and CAC were investigated at different initial concentrations ranging from 100 to 1000 mg/L in three different temperatures (30, 40, and 60 °C). These experiments were carried out at optimum pH values and optimum adsorbent dosages with a stirring speed of 200 rpm for 1 h. The effects of two different operating conditions as temperature and the initial Cu(II) concentrations were presented together. The comparisons of the effects of temperature at pH 5 and pH 7 for PAC and CAC as a function of initial concentration are given in Fig. 3.

From Fig. 3, Cu(II) removal showed the same trend for both adsorbents at pH 5 and 7. Cu(II) removal decreased with an

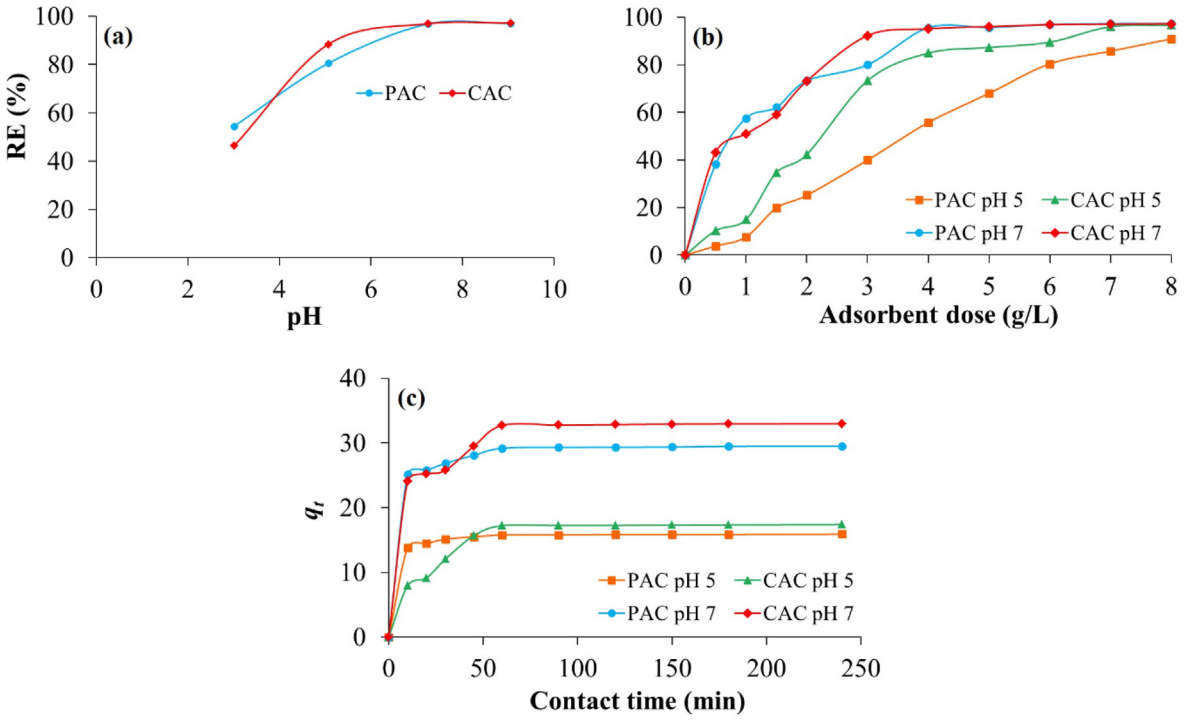

Fig. 2. The comparison of the effects of pH (a), adsorbent dose (b), and contact time (c) on Cu(II) adsorption.

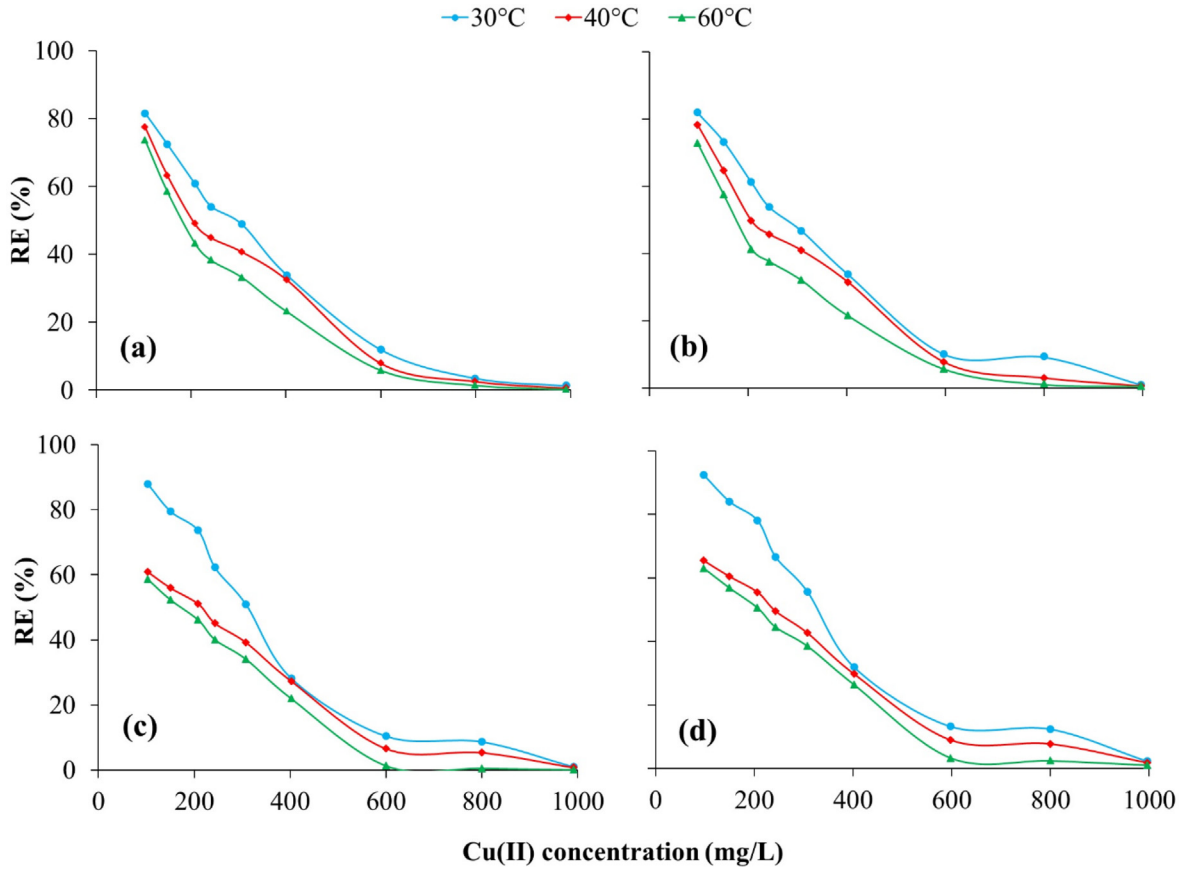

Fig. 3. The comparison of the effects of temperature at pH 5 (a) and pH 7 (b) for PAC and at pH 5 (c) and pH 7 (d) for CAC.

increase in temperature and initial concentration. However, for PAC and CAC, the maximum removal efficiencies were achieved with an initial concentration of 300 mg/L in all trials conducted at pH 5 and 7. The maximum adsorption capacities of PAC for 30, 40, and 60 °C at 300 mg/L of Cu(II) concentration were determined as 25.03 mg/g, 21.71 mg/g, and 17.01 mg/g at pH 5, 47.98 mg/g,

42.12 mg/g and 32.95 at pH 7, respectively. Moreover, the Cu(II) removal of PAC decreased from 49 to 31% at pH 5, and from 47% to 32% at pH 7 as the temperature was increased from 30 °C to 60 °C. The maximum adsorption capacities of CAC for 30, 40, and 60 °C were 26.11 mg/g, 20.11 mg/g, and 17.48 mg/g, and Cu(II) removal was found as 51, 39, and 34% at pH 5, respectively. At pH 7, the maximum adsorption capacities of CAC increased to 57.11 mg/g, 43.82 mg/g, and 39.55 mg/g, and the removal efficiency was achieved 56%, 43%, and 38% for 30 °C, 40 °C, and 60 °C, respectively. Similar results were also reported in Cu(II) removal of cationic surfactant-modified bentonites [62] and natural clay [63] from the aqueous solution by the adsorption process. The removal efficiencies of PAC and CAC decreased with an increase in Cu(II) concentration. Lower removal efficiencies were obtained as a result of the interaction of Cu(II) ions in the solution with the binding sites of the adsorbents and reaching the saturation of the adsorption sites. Therefore, the adsorption performances of adsorbents can be effectively increased by the dilution of wastewater containing high metal concentrations.

Kinetics and isotherms

The adsorption kinetics were tested to understand the adsorption behaviors of PAC and CAC for Cu(II) adsorption by Elovich, intra-particle diffusion, pseudo-first-order, and second-order reaction kinetic models. The constants and correlation coefficients of the kinetic models for Cu(II) adsorption were calculated (see supplementary material). According to the correlation coefficients, the adsorption of Cu(II) was better described by the second-order kinetic model. Similar results were observed in many studies [6,60,62]. The second-order kinetic model depends on the assumption that chemical adsorption is the rate-limiting step in the adsorption process. It is possible to say that the adsorption behavior occurs through electron sharing between metal ions and adsorbents. Consequently, the chemisorption played a dominant role in Cu(II) adsorption onto PAC and CAC. Moreover, the intraparticle diffusion model was applied to investigate the diffusion mechanism of the experimental data. Adsorbate transfer to adsorbents occurs in three stages. These are film diffusion, intraparticle diffusion, and adsorption. If the linear plot of $t^{1/2}$ versus q_t shows multilinearity, more than one step affects the adsorption process. First, adsorbate diffusion takes place from the liquid to the adsorbent surface, followed by the rate-limiting stage of intra-particle diffusion and the final equilibrium stage. The model graphs obtained showed that the adsorption took place in two steps. Table 1 also presents that the intercept (C) values increase with an increase in pH value, but the regression line did not pass through the origin ($C \neq 0$). The deviations from the original mean that the diffusion of Cu(II) ions to the adsorbent pores is not the only determining factor that controlled the adsorption mechanism. Therefore, film diffusion and intraparticle diffusion were effective steps in Cu(II) adsorption on PAC and CAC.

Table 1
A comparison of maximum Cu(II) adsorption capacities of different adsorbents.

Adsorbent	q_m (mg/g)	Reference
Ceratophyllum demersum	6.17	[64]
Myriophyllum spicatum	10.37	[65]
Gracillaria sp.	37.5	[66]
Modified bentonite	50.76	[62]
Natural clay	6.25	[67]
Chitosan/rectorite nano-hybrid composite	20.49	[68]
Chitosan bead-supported $MnFe_2O_4$ nanoparticles	43.94	[16]
Black gram husk	27.7	[69]
Functionalized silica	20.5	[70]
Tectona grandis L.f.	15.43	[61]
PAC	48.31	This study
CAC	45.46	This study

Adsorption isotherms are significant in explaining the interactions between molecules or ions of adsorbate and surface sites of adsorbent. For this, the equilibrium curves are drawn and the most favorable correlation is determined among the isotherm models [47,48]. Langmuir, Freundlich, Tempkin, and Dubinin–Radushkevich isotherm models were used to understand the Cu(II) adsorption mechanism of PAC and CAC. The constants of isotherm models for Cu(II) adsorption were found (see supplementary material). According to the correlation coefficients, the Langmuir isotherm model showed the linear profile with the highest value of R^2 for the adsorption of Cu(II) on PAC and CAC for all temperatures, pH values, and adsorbents ($R^2 > 0.970$). The maximum adsorption capacities, from the Langmuir isotherm for both adsorbents were found at pH 7. However, the maximum adsorption capacities q_m were estimated to be 48.309 mg/g for PAC at 30℃ with 0.996 of R^2 value, while it was determined as 45.455 mg/g for CAC at 40℃ with 0.980 of R^2 value. The separation factor, R_L, provides information about the adsorption nature such as irreversible ($R_L = 0$), favorable ($0 < R_L < 1$), linear ($R_L = 1$), or unfavorable ($R_L > 1$). R_L values between 0 and 1 for both adsorbents at all experimental conditions showed that Cu(II) ions preferred to be attached to the adsorbent surface and the nature of the adsorption process was favorable. Langmuir isotherm is a theoretical model that assumes the adsorbent exhibits a homogeneous surface, and all sites of the adsorbent have an equal affinity with the adsorbate. From the results, Cu(II) adsorption indicates that a homogeneous monolayer formation occurs on the surface of PAC and CAC.

Maximum adsorption capacities of different adsorbents used for Cu(II) adsorption were given in Table 1. PAC and CAC used in this study showed good performance in Cu(II) removal among other adsorbents. According to Table 1, it was seen that *Phragmites australis* had almost the same adsorption capacity as other alternative adsorbents. Therefore, it is understood that *Phragmites australis* can be evaluated in the adsorption process as an alternative material for Cu(II) removal.

Adsorption thermodynamics

The Gibbs free energy change (ΔG°), enthalpy change (ΔH°), and entropy change (ΔS°) are found from the thermal-varying of K_L constant obtained from Langmuir isotherm. The thermodynamic parameters provide information about an isolated system's adsorption behavior and mechanism. ΔG°, ΔH°, and ΔS° values are calculated as follows [61]:

$$\Delta G^{\circ} = -RTlnK_L \tag{14}$$

$$\Delta G^{\circ} = \Delta H^{\circ} - T\Delta S^{\circ} \tag{15}$$

$$lnK_L = \frac{\Delta S^{\circ}}{R} - \frac{\Delta H^{\circ}}{RT} \tag{16}$$

where T is the absolute temperature (K), and R is the universal gas constant (8.314 j / mol K). ΔS° (j/mol K) and ΔH° (kj/mol) are calculated from intercept and slope from Van't Hoff plot that is drawn 1/T versus lnK_L, respectively.

ΔG° provides information about the spontaneity and feasibility of adsorption. A negative value of ΔG° indicates that the adsorption behavior is spontaneous and feasible. ΔG° value, which is more negative with an increase in temperature, increases the spontaneity and feasibility of adsorption. Thus, a more energetic adsorption behavior is observed [71]. ΔH° is an important parameter to determine the type of adsorption (physical or chemical process) [72]. ΔH° is the measure of the energy barrier that the

reacting molecules must overcome. A positive value of ΔH° indicates that the nature of the adsorption process is endothermic. Therefore, external energy input is needed in the adsorption process [73]. On the other hand, a negative value of ΔH° means that the adsorption process has an exothermic nature, and is controlled by a physical mechanism [6]. ΔS° shows the characteristic properties of the reaction (an associative or dissociative mechanism) [74]. A negative ΔS° value presents that the randomness decreases at the adsorbent and adsorbate interface after the adsorption process. If ΔS° is positive, the randomness of the interface increases [18].

The effects of temperature at pH 5 and pH 7 on Cu(II) adsorption of PAC and CAC as a function of initial concentration were performed at 30 °C, 40 °C, and 60 °C. Thermodynamic parameters were determined from Van't Hoff plots (see supplementary material).

ΔG values were from −24.99 to −26.23 kJ/mol for PAC and −5.525 to −10.60 kJ/mol for CAC. Moreover, for PAC, the ΔG value was more negative with an increase in the temperature. For CAC, the ΔG values were negative and decreased with an increase in the temperature. It indicated that the spontaneity and feasibility of Cu(II) adsorption were directly proportional to the temperature, unlike CAC. Thus, it can be said that the adsorption behavior of PAC is more energetic than that of CAC. The enthalpy changes found for PAC and CAC took negative values. ΔH° values were calculated as −12.49 kJ/mol for PAC and −5.38 kJ/mol for CAC. The negative values of ΔH° indicated that Cu(II) adsorption had an exothermic nature, and was controlled by a physical mechanism for both adsorbents. It was determined that the adsorption capacities of both adsorbents decreased relatively with the increase in temperature. This situation can be explained as the weakening of the adsorptive forces between the active sites of the adsorbent and Cu(II) ions [18]. The ΔS° were calculated as 41.26 j/mol K and 17.22 j/mol K for PAC and CAC, respectively. The positive values observed for both adsorbents indicated that after the adsorption process, Cu(II) ions were randomly distributed at the adsorbent and adsorbent interface.

Modeling of Cu(II) adsorption

The modeling of Cu(II) adsorption from synthetic wastewater was carried out via three modeling tools. Two of these are soft computing approaches such as MFIS and FFNN that form the basic focus of this study too. Another one is RSM, which is based on a statistical approach and has some rigid assumptions. In the use of MFIS and FFNN, the datasets were divided into two subsets as training and testing. pH, adsorbent dose, initial concentration, contact time, and temperature were determined as explanatory variables to predict Cu(II) adsorption for each experiment. The summarization of all experiments in the modeling process of Cu (II) adsorption from synthetic wastewater is presented in Table 2.

Evaluation perspectives

In this study, the evaluation perspectives of the obtained results can be subsumed under two points of view: (*i*) comparison in terms of error criteria of root mean square error (RMSE)(Eq. (17)), median absolute percentage error (MdAPE) (Eq. (18)) median absolute error (MdAE) (Eq. (19)), Willmott's Index (WI) (Eq. (20)) [75], and modified index of agreement (md) (Eq. (21)) [76], and (*ii*) investigating some features of a regression model created for the target values and the obtained predictions values (Eq. (22)). The regression and the determination coefficients are produced equal to 1 or very close to 1 for a successful prediction tool. Moreover, it is expected that the confidence interval of the regression coefficient covers 1.

$$RMSE = \sqrt{\frac{1}{n}\sum_{p=1}^{n}\left(Target_p - Output_p\right)^2} \tag{17}$$

$$MdAPE = median\left(\left|\frac{Target_p - Output_p}{Target_p}\right|\right), p = 1, 2, \cdots, n \tag{18}$$

$$MdAE = median\left(\left|Target_p - Output_p\right|\right), p = 1, 2, \cdots, n \tag{19}$$

$$WI = 1 - \frac{\sum_{p=1}^{n}\left|Target_p - Output_p\right|}{\sum_{p=1}^{n}\left|mean(Target) - Output_p\right| + \left|mean(Target) - Target_p\right|}, p = 1, 2, \cdots, n \tag{20}$$

$$md = 1 - \frac{\sum_{p=1}^{n}\left|Target_p - Output_p\right|^j}{\sum_{p=1}^{n}\left(\left|mean(Target) - Output_p\right| + \left|mean(Target) - Target_p\right|\right)^j}, p = 1, 2, \cdots, n \tag{21}$$

$$Y_p = \beta\widehat{Y}_p + \varepsilon_p \tag{22}$$

Comparison of the results via error criteria

RMSE values of the predictors and their performance rankings for this error criterion were calculated (see supplementary material). The soft computing-based MFIS and FFNN produced better predictions for Cu(II) adsorption. When the two soft computing-based models were evaluated within themselves, it was seen that fuzzy-based MFIS outperformed FFNN in 5 of 6 experiments. However, what should not be overlooked was that FFNN also produced successful results at a satisfactory level for all experiments.

Moreover, according to the obtained results in terms of MdAPE and MdAE criteria (see supplementary material), it was seen that in terms of both criteria, soft computing-based models showed better predictive performance than RSM for almost all experiments. Specifically, for experiments 3 and 4, MFIS and FFNN produced predictions with an error of less than 1%. These errors, for experiments 1 and 2, were obtained at a level of less than 5%. Although the errors of experiments 5 and 6 exceeded 5% for the whole data set, they could still be considered reasonable errors and were still much better than the RSM results. Moreover, the reliability and consistency of these models were also proved with the successful performance of the soft computing-based MFIS and FFNN in the test sets of experiments.

Evaluation of the performance via linear regression analyses

From another point of view, some properties of a simple linear regression model can be used as evidence of the superior predictive ability of any prediction tool. At this point, it can be established $Y_t = \beta\widehat{Y}_t + \varepsilon_t$ model and investigated the values of the regression coefficient ($\widehat{\beta}$) and also the determination coefficient R^2. What is desired here is that these coefficients are 1 or very close to 1. Regression models were established for the predictions of soft computing-based models (see supplementary material).

From the shared properties of regression analysis for each experiment, it was clear that both β and R^2 values were fairly close to 1, as expected. It means that the predictions generated by FINN and MFIS are quite in harmony with the actual adsorption rates. On the other hand, 95% confidence intervals of β have a very narrow frame besides they covered 1, as expected again. All these findings regarding regression analysis prove that FFNN and MFIS can be used as elite modeling tools in this prediction problem.

Besides the statistical evidence, some visual graphs can also be used to bring to light the superior performance of the soft

Table 2
The summarization of all experiments in the modeling process of Cu(II) adsorption.

Experiment	Adsorbent	Independent Variables	# of Membership Function	FFNN Architecture
1	PAC	A. pH Adsorbent dose Initial concentration	3	from 3-1-1 to 3–3-1
2	CAC	pH Adsorbent dose Initial concentration		
3	PAC	A. pH Contact time Initial concentration		
4	CAC	A. pH Contact time Initial concentration		
5	PAC	A. pH Temperature Initial concentration		
6	CAC	A. pH Temperature Initial concentration		

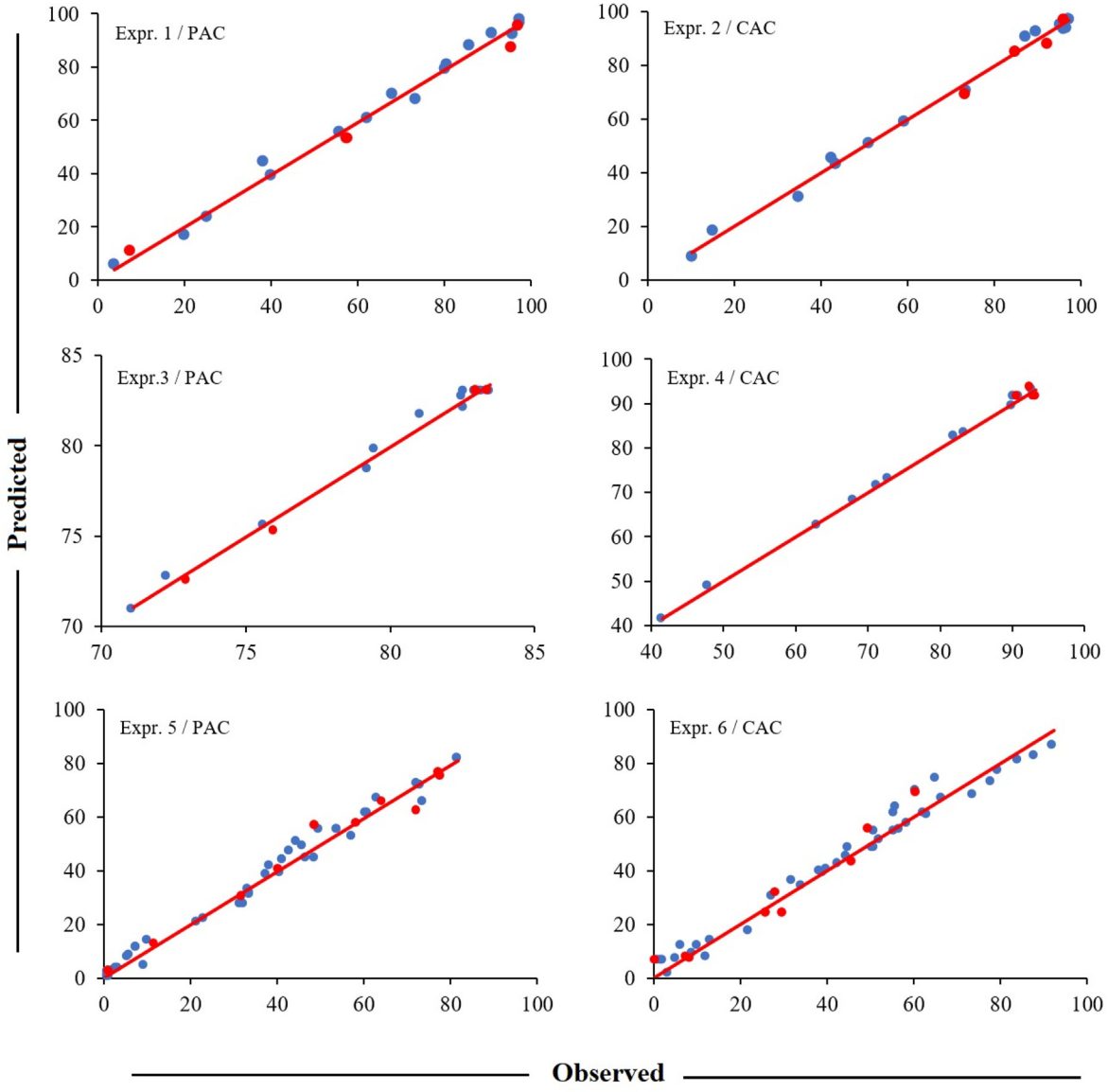

Fig. 4. The scatter plots of actual and predicted adsorption performance for FFNN.

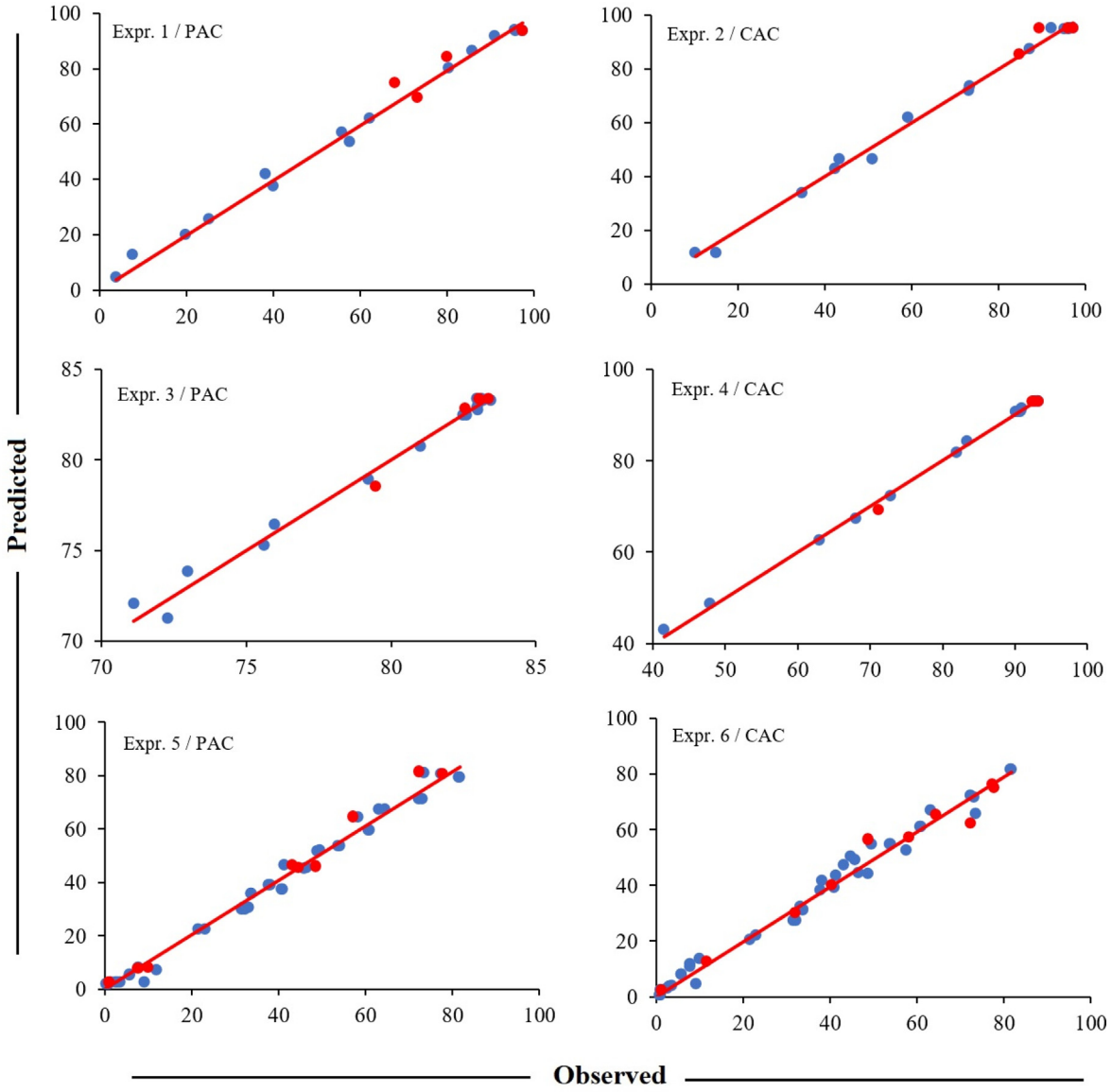

Fig. 5. The scatter plots of actual and predicted adsorption performance for MFIS.

computation-based models used in this study. A scatter plot is one of them. The scatter plot is a mathematical diagram using cartesian coordinates. In the scatter plot, it is desired that most of the points constituted by the observed and predicted adsorption rate values need to be close to a line segment. The scatter graphs established for two soft computing modeling tools are given in Figs. 4 and 5.

From the figures, the points formed by the observed and predicted adsorption values are spread almost straight. This can be considered as further proof of the superior performances of FFNN and MFIS.

Moreover, the performance of the models can be evaluated by Heat map, Taylor diagram, Box plot, and Violin plot given in Fig. 6. Heat map uses to present six performance metrics. Taylor diagram presents three models to exhibit the closeness between actual and predicted values using standard deviation and correlation values.

The box plot shows a residual error of three models to demonstrate the IQR and its characteristics. Violin plots visualize the size of the violin, IQR, and its characteristics of the box plot for the distribution of actual and predicted values by three models. As an exemplary evaluation, the results obtained from experiments 3 and 4 modeling process were evaluated by considering these graphs.

From the heat-map given in Fig. 6(a), it was seen that R^2, *WI* and *md* metrics obtained from the MFIS and the FFNN were quite close to 1 (the region represented in yellow) by the side of the RSM. Additionally, in terms of RMSE, MdAPE, and MdAE metrics, MFIS and the FFNN produced values close to 0 (the region represented in orange) compared to the RSM. Thus, the heat-map created for all performance metrics proved that the soft computing-based models outperformed RSM. Another way to visually investigate the predictive performance of models is to draw a Taylor diagram, given in Fig. 6(b) that presents correlations between actual and predicted values besides the standard deviations (SDs). Taylor's diagram showed that the SDs of predictions obtained from the FFNN (green point) and the MFIS (blue point) were quite close to the SD of actual observations in comparison with the RSM (pink point). Moreover, the correlation values obtained for the FFNN and the MFIS were over 0.99, while this value was about 0.90 for RSM. In that way, it was seen that the Taylor diagram contained

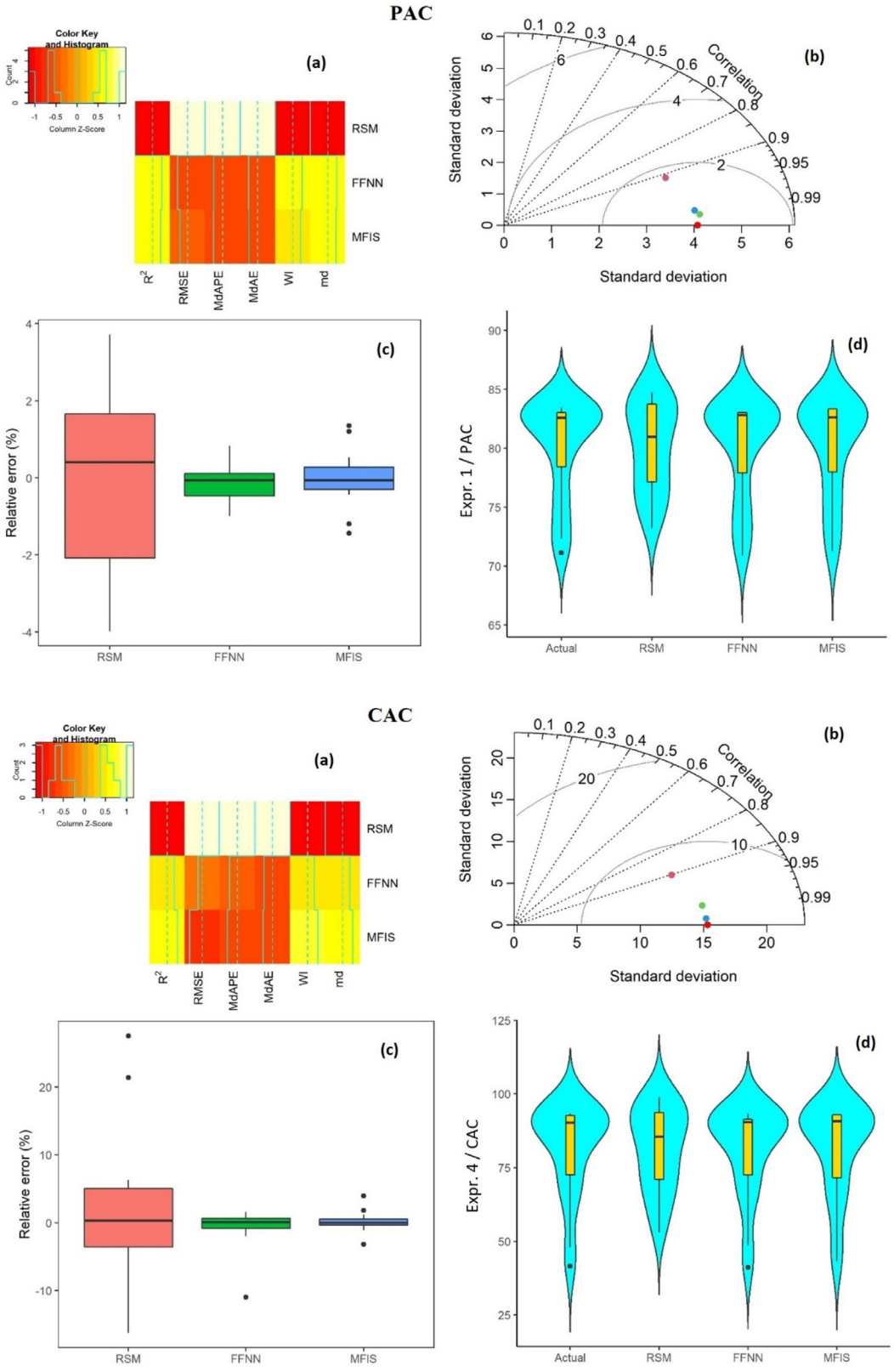

Fig. 6. Heat map (a), Taylor diagram (b), Box plot (c), and Violin plot (d) for Expr. 3 results of PAC adsorption and Expr. 4 of CAC adsorption.

visual findings to prove the superiority of FFNN and MFIS models over RSM.

Also, the box plot (Fig. 6(c)) can be used to validate the predictive ability of the models in terms of reliability and validity. In the box plot, RSM had the largest interquartile range (IQR), the largest maximal relative errors (REs), and the least minimal RE by the side of the FFNN and the MFIS. But the FFNN and the MFIS had a fairly narrow IQR, fairly small maximal REs, and fairly large minimal REs.

Table 3
The findings of the optimization process.

Exp.	Adsorbent	Constraints	Optimal Values	Target Values	Objective Function Values	Desirability	Predictor
1	PAC	$5 \leq pH \leq 70.50 \leq Adsorbentdose \leq 8.0096.40 \leq Co \leq 100.40$	6.9997 6.0019 96.6064	97.3205	93.9570	96.40%	**MFIS**
2	CAC	$5 \leq pH \leq 70.50 \leq Adsorbentdose \leq 8.0091.30 \leq Co \leq 96.40$	6.1217 7.8115 96.1559	97.2095	95.0360	97.50%	
3	PAC	$5 \leq pH \leq 710 \leq Contacttime \leq 240106.00 \leq Co \leq 114.60$	6.7510 124.8334 105.8368	83.4623	83.3517	99.10%	
4	CAC	$5 \leq pH \leq 710 \leq Contacttime \leq 240106.00 \leq Co \leq 114.60$	6.9998 159.5129 105.9991	93.2830	92.8854	99.23%	
5	PAC	$5 \leq pH \leq 730 \leq Temperature \leq 6098.20 \leq Co \leq 996.50$	5.0000 59.0844 98.2000	81.6904	81.0654	99.23%	
6	CAC	$5 \leq pH \leq 730 \leq Temperature \leq 6098.20 \leq Co \leq 996.50$	5.0000 30.0000 98.2000	92.3320	85.3078	92.38%	
1	PAC	$5 \leq pH \leq 70.50 \leq Adsorbentdose \leq 8.0096.40 \leq Co \leq 100.40$	5.0144 7.9998 96.6064	97.3205	93.5317	95.95%	**FFNN**
2	CAC	$5 \leq pH \leq 70.50 \leq Adsorbentdose \leq 8.0091.30 \leq Co \leq 96.40$	6.9937 7.0365 96.3973	97.2095	97.1466	99.93%	
3	PAC	$5 \leq pH \leq 710 \leq Contacttime \leq 240106.00 \leq Co \leq 114.60$	6.9980 239.1680 114.5570	83.4623	83.0248	96.46%	
4	CAC	$5 \leq pH \leq 710 \leq Contacttime \leq 240106.00 \leq Co \leq 114.60$	6.9976 76.8590 106.0510	93.2830	94.0794	100.00%	
5	PAC	$5 \leq pH \leq 730 \leq Temperature \leq 6098.20 \leq Co \leq 996.50$	5.1271 30.0000 360.0732	81.6904	99.9318	100.00%	
6	CAC	$5 \leq pH \leq 730 \leq Temperature \leq 6098.20 \leq Co \leq 996.50$	6.9999 30.0000 98.2000	92.3320	86.1685	93.32%	

From this point of view, it was said that FFNN and MFIS performed much more reliably and much more valid performance compared to RSM.

Finally, the harmony of distribution for the actual observation and predictions can be observable by a violin plot given in Fig. 6 (d). The harmony of distribution for the actual observation and predictions can be observable by a violin plot given in Fig. 6(d). These violin plots clearly showed that, in comparison with the RSM, the predicted values obtained from the FFNN and the MFIS were remarkably nearer to the actual values.

Optimization via genetic algorithm

This study suggests the usage of FFNN and MFIS as soft computing approaches to predict Cu(II) adsorption from synthetic wastewater. The usage of such predictors is crucial for experimental design and the prediction of the response variable. However, perhaps it is most important to determine for which input values these estimators will produce the maximum or minimum response. Because such an acquisition often enables the optimal response variable value to be obtained without performing new experiments, which can be very costly and time-consuming. The input parameters were optimized by the genetic algorithm which is another soft computing tool. The objective function can be given as follows:

$$y = f(X_1, X_2, X_3) \tag{23}$$

In Eq. (23), $X_1, X_2,$ and X_3 are the input parameters of the adsorption process. y is the response variable i.e., it depicts the adsorption rate (%) adsorption from synthetic wastewater. Also, f is a predictor.

Table 3 recapitulates the findings of the optimization process. GA for both software-based prediction tools reached the desirability ratios of over 95% except for just two experiments. For example, for the MFIS, for experiment 2 with the pH of 6.1217, adsorption dose of 7.8115, and initial concentration of 96.1559 mg/L, the optimized condition leads to maximum Cu(II) removal (95.0360%) with 97.50% desirability. These ratios even are 100% for two experiments. These desirability rates show once again that two soft computing-based prediction tools can be used with confidence to predict Cu(II) adsorption. Moreover, these findings also prove that these prediction tools are functions for predicting the maximum adsorption performance.

Hypothesis tests

Considering the results of the optimization transaction in detail, although CAC, under the optimum conditions, had higher adsorption performance against PAC, this situation was needing proof by statistical hypothesis tests. The adsorption performances of CAC and PAC were statistically evaluated with the test of independent samples (see supplementary material).

Investigating these results can be done in two ways. The first is to evaluate the p values, and the second is to consider the 95% confidence interval of the differences. In the first, all p-values were greater than 0.05. In the second, all of the 95% confidence intervals of the differences involved the zero value. These findings were evidence that there was no significant difference between the adsorption performances of CAC and PAC for all experiments.

Conclusions

In this study, Cu(II) adsorption performances of activated Phragmites australis waste and commercial activated carbon were modeled by soft computing models. The adsorption kinetics and isotherms were tested and presented the best conformity pseudo-second-order reaction kinetic and Langmuir isotherm models. It means that the rate-limiting step is chemisorption rather than diffusion and a homogeneous monolayer formation of Cu(II) occurs on the surface of adsorbents. According to the thermodynamic parameters, Cu(II) adsorption of both adsorbents had an exothermic nature and the product was energetically stable and indicated increasing randomness.

The superior modeling performances of the soft computation-based approaches were demonstrated by the great harmony between predicted and observed Cu(II) adsorption. MFIS and FFNN performed exceptionally well with a relative error of less than 2–3% in the first four experiments, while in the remaining two experiments these tools again showed successful modeling with a relative error of 6–7%. These findings are supported by two parameters ($\widehat{\beta}$ and R^2) whose values were very close to one, obtained from the regression models created for the real CU(II) with the predictions. Moreover, all 95% confidence intervals for beta include one. In terms of the coefficient of determination, it is seen that this study performs better (with over 99% R^2 values) than the studies presenting the linear model (under 99% R^2 values).

In terms of adsorption performances under optimum conditions, although CAC was more successful than PAC, no statistical difference was found in Cu(II) removal performances (all 95% confidence intervals cover zero**)**. However, two soft computing-based predictors, MFIS and FFNN, can be confidently used to predict Cu (II) adsorption. In optimization of the simulation of the Cu(II) adsorption process activated by PAC and CAC, desirability levels of over 95% were achieved in 5 of 6 experiments for both PCA and CAC. For a single remaining experiment, the desirability rate was over 90%. Therefore, optimal conditions for experimental design can be determined by GA without additional experiments for another soft computing-based approach. The fact that both MFIS and FFNN are data-driven models means that their performance is specific to these datasets. Moreover, the random start also creates a limitation on their success. These limitations do not mean that they are not a successful modeling tool, and they can be investigated from another perspective in another study.

Declaration of Competing Interest

The authors declare that they have no known competing financial interests or personal relationships that could have appeared to influence the work reported in this paper.

Appendix A. Supplementary material

Supplementary data to this article can be found online at https://doi.org/10.1016/j.jiec.2023.08.031.

References

[1] M. Ajmal, A. Hussain Khan, S. Ahmad, A. Ahmad, Water Res. 32 (10) (1998) 3085–3091, https://doi.org/10.1016/S0043-1354(98)00067-0.
[2] G. Dönmez, Z. Aksu, Process Biochem. 35 (1–2) (1999) 135–142, https://doi.org/10.1016/S0032-9592(99)00044-8.
[3] A. Özer, G. Gürbüz, A. Çalimli, B.K. Körbahti, Chem. Eng. J. 146 (3) (2009) 377–387, https://doi.org/10.1016/j.cej.2008.06.041.
[4] S. Chatterjee, S. Mondal, S. De, J. Clean. Prod. 177 (2018) 760–774, https://doi.org/10.1016/j.jclepro.2017.12.249.
[5] R. Upadhyay, P.K. Pandey, Pardeep, Mater. Today:. Proc. 4 (9) (2017) 10504–10508, https://doi.org/10.1016/j.matpr.2017.06.409.
6 F. Aydın Temel, Int. J. Exergy 23 (4) (2017) 279–297, https://doi.org/10.1504/IJEX.2017.086168.
[7] H. Benaïssa, M.A. Elouchdi, Chem. Eng. Process. 46 (7) (2007) 614–622, https://doi.org/10.1016/j.cep.2006.08.006.
[8] S.R. Shukla, R.S. Pai, Sep. Purif. Technol. 43 (1) (2005) 1–8, https://doi.org/10.1016/j.seppur.2004.09.003.
[9] F. Güzel, H. Yakut, G. Topal, J. Hazard. Mater. 153 (2008) 1275–1287.
[10] T. Salman, F. Aydın Temel, G. Turan, Y. Ardalı, Desalin. Water Treat. 56 (2014) 1566–1575, https://doi.org/10.1080/19443994.2014.951073.
[11] M. Alkan, B. Kalay, M. Doğan, Ö. Demirbaş, J. Hazard. Mater. 153 (1–2) (2008) 867–876, https://doi.org/10.1016/j.jhazmat.2007.09.047.
[12] A. Azari, A. Mesdaghinia, G. Ghanizadeh, H. Masoumbeigi, M. Pirsaheb, H.R. Ghafari, T. Khosravi, K. Sharafi, Water Sci. Technol. 74 (6) (2016) 1446–1456, https://doi.org/10.2166/wst.2016.318.
[13] M.H. Mahmoudian, M. Fazlzadeh, M.H. Niari, A. Azari, E.C. Lima, Arab. J. Chem. 13 (9) (2020) 7147–7159, https://doi.org/10.1016/j.arabjc.2020.07.020.
[14] M.A. Shaker, A.A. Yakout, Spectrochim. Acta - Part A Mol. Biomol. Spectrosc. 154 (2016) 145–156, https://doi.org/10.1016/j.saa.2015.10.027.
[15] N.G. Apostol, M.A. Husanu, D. Lizzit, I.A. Hristea, C.F. Chirilă, L. Trupină, C.M. Teodorescu, Catal. Today 366 (January 2020) (2021) 141–154, https://doi.org/10.1016/j.cattod.2020.02.042.
[16] H. Li, H. Ji, X. Cui, X. Che, Q. Zhang, J. Zhong, R. Jin, L. Wang, Y. Luo, Int. J. Min. Sci. Technol. (2021), https://doi.org/10.1016/j.ijmst.2021.10.004.
[17] J. Jaafari, M.G. Ghozikali, A. Azari, M.B. Delkhosh, A.B. Javid, A.A. Mohammadi, S. Agarwal, V.K. Gupta, M. Sillanpää, A.G. Tkachev, A.E. Burakov, J. Ind. Eng. Chem. 57 (2018) 396–404, https://doi.org/10.1016/j.jiec.2017.08.048.
18 H. Cüce, F. Aydın Temel, Int. J. Glob. Warm. 24 (1) (2021) 14–37, https://doi.org/10.1504/ijgw.2021.115108.
[19] N.K. Soliman, A.F. Moustafa, A.A. Aboud, K.S.A. Halim, J. Mater. Res. Technol. 8 (2) (2019) 1798–1808, https://doi.org/10.1016/j.jmrt.2018.12.010.
[20] A. Stavrinou, C.A. Aggelopoulos, C.D. Tsakiroglou, J. Environ. Chem. Eng. 6 (6) (2018) 6958–6970, https://doi.org/10.1016/j.jece.2018.10.063.
[21] K.A. Adegoke, O.S. Bello, Water Resour. Ind. 12 (2015) 8–24, https://doi.org/10.1016/j.wri.2015.09.002.
[22] M.J. Ahmed, Ecol. Eng. 102 (2017) 262–269, https://doi.org/10.1016/j.ecoleng.2017.01.047.
[23] M.A. Yahya, Z. Al-Qodah, C.W.Z. Ngah, Renew. Sustain. Energy Rev. 46 (2015) 218–235, https://doi.org/10.1016/j.rser.2015.02.051.
[24] M.J. Ahmed, J. Environ. Chem. Eng. 4 (1) (2016) 89–99, https://doi.org/10.1016/j.jece.2015.10.027.
[25] M.A. Zazouli, A. Azari, S. Dehghan, R.S. Malekkolae, Water Sci. Technol. 74 (9) (2016) 2021–2035, https://doi.org/10.2166/wst.2016.287.
[26] F. Barjasteh-Askari, M. Davoudi, M. Dolatabadi, S. Ahmadzadeh, Heliyon 7 (6) (2021) e07191.
[27] M. Dolatabadi, H. Naidu, S. Ahmadzadeh, J. Clean. Prod. 316 (July) (2021), https://doi.org/10.1016/j.jclepro.2021.128226.
[28] G.D. Noudeh, M. Asdaghi, N.D. Noudeh, M. Dolatabadi, S. Ahmadzadeh, Environ. Monit. Assess. 195 (1) (2023) 1–12, https://doi.org/10.1007/s10661-022-10808-z.
[29] M. Dolatabadi, A. Kheirieh, M. Yoosefian, S. Ahmadzadeh, Appl. Water Sci. 12 (11) (2022) 1–9, https://doi.org/10.1007/s13201-022-01780-7.
[30] O. Cagcag Yolcu, E. Bas, E. Egrioglu, U. Yolcu, Neural Process. Lett. 47 (3) (2018) 1133–1147, https://doi.org/10.1007/s11063-017-9686-3.
31 U. Yolcu, E. Egrioglu, E. Bas, O. Cagcag Yolcu, A.Z. Dalar, J. Exp. Theor. Artif. Intell. 33 (3) (2021) 383–404, https://doi.org/10.1080/0952813X.2019.1595167.
[32] N.G. Turan, B. Mesci, O. Ozgonenel, Chem. Eng. J. 171 (3) (2011) 1091–1097, https://doi.org/10.1016/j.cej.2011.05.005.
[33] N.G. Turan, B. Mesci, O. Ozgonenel, Chem. Eng. J. 173 (1) (2011) 98–105, https://doi.org/10.1016/j.cej.2011.07.042.
[34] S.M.H. Asl, M. Ahmadi, M. Ghiasvand, A. Tardast, R. Katal, J. Ind. Eng. Chem. 19 (3) (2013) 1044–1055, https://doi.org/10.1016/j.jiec.2012.12.001.
[35] O. Cagcag Yolcu, F. Aydın Temel, A. Kuleyin, J. Clean. Prod. 311 (May) (2021), https://doi.org/10.1016/j.jclepro.2021.127688.
36 F. Aydın Temel, O. Cagcag Yolcu, A. Kuleyin, J. Hazard. Mater. 410 (September) (2021), https://doi.org/10.1016/j.jhazmat.2020.124670.
[37] C.A. Igwegbe, L. Mohmmadi, S. Ahmadi, A. Rahdar, D. Khadkhodaiy, R. Dehghani, S. Rahdar, MethodsX 6 (2019) 1779–1797, https://doi.org/10.1016/j.mex.2019.07.016.
[38] M.R. Gadekar, M.M. Ahammed, J. Environ. Manage. 231 (October 2018) (2019) 241–248, https://doi.org/10.1016/j.jenvman.2018.10.017.
[39] M. Maghsoudi, M. Ghaedi, A. Zinali, A.M. Ghaedi, M.H. Habibi, Spectrochim. Acta - Part A Mol. Biomol. Spectrosc. 134 (2015) 1–9, https://doi.org/10.1016/j.saa.2014.06.106.
[40] M. Ghaedi, R. Hosaininia, A.M. Ghaedi, A. Vafaei, F. Taghizadeh, Spectrochim. Acta - Part A Mol. Biomol. Spectrosc. 131 (2014) 606–614, https://doi.org/10.1016/j.saa.2014.03.055.
[41] K. Aghajani, H.A. Tayebi, Spectrochim. Acta - Part A Mol. Biomol. Spectrosc. 171 (2017) 439–448, https://doi.org/10.1016/j.saa.2016.08.025.
[42] H. Javadian, S. Asadollahpour, M. Ruiz, A.M. Sastre, M. Ghasemi, S.M.H. Asl, M. Masomi, J. Taiwan Inst. Chem. Eng. 91 (2018) 186–199, https://doi.org/10.1016/j.jtice.2018.06.021.
[43] S. Anbazhagan, V. Thiruvengadam, K. Kulanthai, Iran. J. Chem. Chem. Eng. 39 (6) (2020) 75–93, https://doi.org/10.30492/ijcce.2019.36407.
[44] H. Yiğit, Production of activated carbon from sunflower meal by hydrothermal carbonization and NaOH activation and investigation of its adsorption

properties. MSc thesis, Department of Chemical Engineering, Ondokuz Mayıs University, Samsun, Turkey, 2017.
[45] S. Wan, Z. Hua, L. Sun, X. Bai, L. Liang, Process Saf. Environ. Prot. 104 (2016) 422–435, https://doi.org/10.1016/j.psep.2016.10.001.
[46] N.G. Turan, O. Ozgonenel, J. Taiwan Inst. Chem. Eng. 44 (6) (2013) 895–903, https://doi.org/10.1016/j.jtice.2013.03.004.
[47] F. Aydın Temel, A. Kuleyin, Desalin. Water Treat. 57 (2016) 23873–23892, https://doi.org/10.1080/19443994.2015.1136964.
[48] Y. Chen, D. Zhang, Chem. Eng. J. 254 (2014) 579–585, https://doi.org/10.1016/j.cej.2014.05.120.
[49] A. Olgun, N. Atar, J. Ind. Eng. Chem. 18 (5) (2012) 1751–1757, https://doi.org/10.1016/j.jiec.2012.03.020.
[50] A. Kuleyin, F. Aydın, Environ. Prog. Sustain. Energy 30 (2) (2011) 141–151, https://doi.org/10.1002/ep.
[51] L.A. Zadeh, IEEE Softw. 11 (6) (1994) 48–56.
[52] D. Ibrahim, Procedia Comput. Sci. 102 (August) (2016) 34–38, https://doi.org/10.1016/j.procs.2016.09.366.
[53] P.J. Werbos, The Roots of Backpropagation, John Wiley & Sons, New York, 1974.
[54] E. Rumelhart,, G. Hinton, R. Williams, The M.I.T. Press, Cambridge, 1986, pp. 318–362.
[55] E.H. Mamdani, Proc. Inst. Electr. Eng. 121 (12) (1974) 1585–1588, https://doi.org/10.1049/piee.1974.0328.
[56] J.H. Holland, Adaptation in Natural and Artificial Systems, University of Michigan Press, Ann Anbor, 1975.
[57] K. De Jong, Analysis of the Behaviour of a Class of Genetic Adaptive Systems. University of Michigan, Ann Arbor, MI, 1975.
[58] A. Özer, D. Özer, A. Özer, Process Biochem. 39 (12) (2004) 2183–2191, https://doi.org/10.1016/j.procbio.2003.11.008.
[59] N. Korboulewsky, R. Wang, V. Baldy, Bioresour. Technol. 105 (2012) 9–14, https://doi.org/10.1016/j.biortech.2011.11.037.
[60] Y. Abdellaoui, M.T. Olguín, M. Abatal, B. Ali, S.E. Díaz Méndez, A.A. Santiago, Superlattice. Microst. 127 (2019) 165–175, https://doi.org/10.1016/j.spmi.2017.11.061.
[61] Y. Prasanna Kumar, P. King, V.S.R.K. Prasad, J. Hazard. Mater. 137 (2) (2006) 1211–1217, https://doi.org/10.1016/j.jhazmat.2006.04.006.
[62] K. Tohdee, L. Kaewsichan, Asadullah, J. Environ. Chem. Eng. 6 (2) (2018) 2821–2828, https://doi.org/10.1016/j.jece.2018.04.030.
[63] S. Veli, B. Alyüz, J. Hazard. Mater. 149 (1) (2007) 226–233, https://doi.org/10.1016/j.jhazmat.2007.04.109.
[64] O. Keskinkan, M.Z.L. Goksu, M. Basibuyuk, C.F. Forster, Bioresour. Technol. 92 (2) (2004) 197–200, https://doi.org/10.1016/j.biortech.2003.07.011.
[65] O. Keskinkan, M.Z.L. Goksu, A. Yuceer, M. Basibuyuk, C.F. Forster, Process Biochem. 39 (2) (2003) 179–183, https://doi.org/10.1016/S0032-9592(03)00045-1.
[66] P.X. Sheng, Y.P. Ting, J.P. Chen, L. Hong, J. Colloid Interface Sci. 275 (1) (2004) 131–141, https://doi.org/10.1016/j.jcis.2004.01.036.
[67] H. Es-Sahbany, R. Hsissou, M.L. El Hachimi, M. Allaoui, S. Nkhili, M.S. Elyoubi, Mater. Today:. Proc. 45 (2021) 7290–7298, https://doi.org/10.1016/j.matpr.2020.12.1100.
[68] L. Zeng, Y. Chen, Q. Zhang, X. Guo, Y. Peng, H. Xiao, X. Chen, J. Luo, Carbohydr. Polym. 130 (2015) 333–343, https://doi.org/10.1016/j.carbpol.2015.05.015.
[69] A. Saeed, M. Iqbal, M.W. Akhtar, J. Hazard. Mater. 117 (1) (2005) 65–73, https://doi.org/10.1016/j.jhazmat.2004.09.008.
[70] M. Güçoğlu, N. Şatıroğlu, J. Mol. Liq. 348 (2022), https://doi.org/10.1016/j.molliq.2021.118388.
[71] N. Boujelben, J. Bouzid, Z. Elouear, J. Hazard. Mater. 163 (1) (2009) 376–382, https://doi.org/10.1016/j.jhazmat.2008.06.128.
[72] M.E. Argun, J. Hazard. Mater. 150 (3) (2008) 587–595, https://doi.org/10.1016/j.jhazmat.2007.05.008.
[73] S. Madala, S.K. Nadavala, S. Vudagandla, V.M. Boddu, K. Abburi, Arab. J. Chem. (2013), https://doi.org/10.1016/j.arabjc.2013.07.017.
[74] I. Mobasherpour, E. Salahi, M. Ebrahimi, J. Saudi Chem. Soc. (2011), https://doi.org/10.1016/j.jscs.2011.09.006.
[75] C. Willmott, S. Ackleson, R. Davis, J. Feddema, K. Klink, D. Legates, J. O'Donnell, C. Rowe, J. Geophys. Res. 90 (C5) (1985) 8995–9005.
[76] G.J.M. David, R Legates, 35(1) (2007) 1–9.